Available online at www.sciencedirect.com
ScienceDirect
Earth and Planetary Science Letters 250 (2006) 428–443
EPSL
www.elsevier.com/locate/epsl

Lithium isotope fractionation in the southern Cascadia subduction zone

Tomáš Magna [a,*], Uwe Wiechert [a,b], Timothy L. Grove [c], Alex N. Halliday [d]

[a] Institute of Isotope Geochemistry and Mineral Resources, ETH Zürich, Clausiusstrasse 25, CH-8092, Zürich, Switzerland
[b] Institut für Geologische Wissenschaften, AB Geochemie/Mineralogie-Petrologie, Freie Universität Berlin, Malteserstrasse 74-100, Haus B204, D-12249 Berlin, Germany
[c] Department of Earth, Atmospheric and Planetary Sciences, Massachusetts Institute of Technology, Cambridge, MA 02139, USA
[d] Department of Earth Sciences, University of Oxford, Park Road, Oxford, OX1 3PR, United Kingdom

Received 15 March 2006; received in revised form 23 August 2006; accepted 23 August 2006
Available online 28 September 2006
Editor: G.D. Price

Abstract

We present lithium (Li) abundances and isotope compositions for a suite of anhydrous olivine tholeiites (HAOTs) and hydrous basalt-andesitic (BA) lavas from the Mt. Shasta and Medicine Lake regions, California. The values of δ^7Li vary from +0.9‰ to +6.4‰ and correlate inversely with distance from the trench. These data are consistent with continuous isotope fractionation of Li during dehydration of the subducted oceanic lithosphere, an interpretation corroborated by uniformly high pre-eruptive H_2O contents in basaltic andesites accompanied by high Li, Rb, Sr, Ba and Pb abundances. The subduction-derived component that was added to these hydrous magmas is shown to be very similar beneath both Mt. Shasta and Medicine Lake volcanoes despite characteristically distinct Li isotope compositions in the magmas themselves. More evolved andesites and dacites from Mt. Shasta have δ^7Li from +2.8 to +6.9‰ which is identical with the range obtained for HAOTs and BA lavas from Mt. Shasta. Therefore, Li isotopes do not provide evidence for any other crustal component admixed to Mt. Shasta andesites or dacites during magmatic differentiation and magma mixing in the crust.

Keywords: lithium isotopes; fluids; subduction zone; mantle wedge; isotope fractionation; Mt. Shasta region

1. Introduction

At convergent plate boundaries cold and brittle oceanic lithosphere descends into the more ductile asthenospheric mantle resulting in explosive volcanism, high-magnitude earthquakes and fast morphological evolution of the overriding plate. Several processes may ultimately lead to melt production: (i) percolation of aqueous slab fluids into the mantle wedge [1,2], (ii) partial melting of the slab [3], (iii) reaction of slab melts

* Corresponding author. Present address: Department of Mineralogy, University of Geneva, Rue des Maraîchers 13, CH-1205 Genève, Switzerland. Tel.: +41 21 692 4364; fax: +41 21 692 4305.
E-mail addresses: magna@erdw.ethz.ch, Tomas.Magna@terre.unige.ch (T. Magna), wiechert@zedat.fu-berlin.de (U. Wiechert), tlgrove@mit.edu (T.L. Grove), alexh@earth.ox.ac.uk (A.N. Halliday).

0012-821X/$ - see front matter © 2006 Elsevier B.V. All rights reserved.
doi:10.1016/j.epsl.2006.08.019

generated by partial melting of the subducted slab with the overlying mantle [4,5], or (iv) more complicated two-step processes such as hydrous metasomatism of cold lithosphere and subsequent melting of "wet" mantle segments related to back-arc rifting [6].

Lithium isotope fractionation is mainly related to low temperature processes at the surface and provides a geochemical tracer of recycled crust in volcanic rocks. Volcanism in the Cascadian arc in California is dominated by basalts with subordinate andesitic to dacitic lavas [7,8]. These evolved lavas are multi-component mixtures of mantle melts and andesite, dacite and rhyodacite magmas produced by fractional crystallization. The high-alumina olivine tholeiites (HAOTs) and basalt-andesitic (BA) lavas of this study do not show a strong overprint of fractional crystallization, crustal contamination and/or magma mixing, making them excellent samples for studying processes in subduction zones [2].

Lithium exhibits large isotope fractionation in the subduction zone environment [9–11]. Generally, it is believed that heavy isotope inputs are provided into the subduction zone by serpentinized peridotites that may have δ^7Li values as heavy as +20‰ [12,13] and altered oceanic basalts [14–16]. Altered seafloor is substantially enriched in Li over fresh ridge basalts to as much as ~80 ppm accompanied by distinctly heavy isotope compositions ~+14‰ [14,15,17]. However, the concept that heavy Li is transferred into the subduction zone environment has been recently questioned because of the light or "mantle-like" δ^7Li values (mainly between −1 and +5‰) found in pelagic clays, oozes, muds and claystones [18] combined with the observation that arc lavas have predominantly MORB-like Li isotope ratios [19]. Progressive shifts toward very negative δ^7Li had been already recognized and were related to preferential loss of ^{7}Li into the fluid phase leaving the residue isotopically light [9]. Indeed, the extent of depletion in ^{7}Li is greater with larger degrees of seafloor alteration. However, the behaviour of Li in subduction zones still remains largely unexplored and rather ambiguous Li cross-arc trends (i.e. linked or not linked to the fluid expulsion from subducted slab) were revealed in various subduction zones and volcanic arcs, e.g. Japan [10,20], northern Cascades [21], Mariana arc [13], Kurile, Aleutian and Sunda arcs [19], Central American Volcanic Arc — CAVA [11,22] or Panama arc [23]. It is thought that the initiation of slab melting may produce extremely light Li isotope compositions [24].

In this paper Li abundances and isotope data are presented for HAOTs and primitive BA lavas from Mt. Shasta and the Medicine Lake regions, northern California. These data are used to place new constraints on the Li isotope geochemistry of convergent plate margins and the inputs of Li to the source of arc volcanics.

2. Geology of the region

Mt. Shasta lies near the southern end of the Cascades chain and is flanked to the west by pre-Tertiary rocks of the Klamath Mountains province. In the northeast and east Mt. Shasta is bordered by Tertiary and Quaternary volcanics of the High Cascades. Medicine Lake lies about 60 km to the east. This back-arc shield volcano has erupted large amounts of basaltic to rhyolitic volcanics. The Lassen Volcanic Field is ~130 km to the south. Tertiary sandstones, shales, and andesitic volcanics, Mesozoic granitic rocks of the Trinity ophiolite and Mesozoic and Palaeozoic meta-sedimentary rocks are present in the Mt. Shasta region and have been inferred to be present beneath the volcano [25].

Subduction zone volcanism in northern California is related to the Juan de Fuca plate, which is being subducted at a half spreading rate of 40 mm/yr [26]. The location of the subducted slab can be estimated at ~110 km depth below Mt. Shasta and has been inferred to be at ~200 km depth below the Medicine Lake region [27–29]. The age of the oceanic plate beneath Mt. Shasta is inferred to be 12–14 Ma [30]. Four major eruptive phases comprise the volcano, Sargents Ridge (<250–130 ka), Misery Hill (80–10 ka), Shastina (10–9.4 ka) and Hotlum (6–2 ka; [31]). Previous geochemical and petrologic studies of Mt. Shasta include those of, for example, Anderson [32].

Some of the samples from this study have been characterized by Grove et al. [2,33,34], Baker et al. [35], Kinzler et al. [36], Wagner et al. [37] and Elkins Tanton et al. [38]. The reader is directed to these authors for further petrologic and geochemical descriptions. The suite of samples comprises two Mt. Shasta and six Medicine Lake primitive high-alumina olivine tholeiites (HAOTs), four basaltic andesites (BA) and one primitive magnesian andesite (PMA) from Mt. Shasta and two basaltic andesites and two samples of the Lake Basalt [37] from Medicine Lake. Additionally, we have analysed six andesites and eight dacites from the Mt. Shasta stratocone.

3. Analytical techniques

Samples were digested in a mixture of doubly distilled concentrated HF and HNO_3 (6:1 by volume), evaporated to dryness and treated three times with

concentrated HNO_3. Subsequently the samples were dissolved in 6 M HCl and loaded on columns. A single step of ion exchange chromatography (BioRad AG50W-X8, 200–400 mesh) was used to separate Li from matrix elements, using 1 M HNO_3 made up in 80%-methanol as elution media. A detailed description of the method is given in Magna et al. [39]. The purified Li solutions were measured on the large-geometry high-resolution multiple-collector ICPMS Nu1700 (Nu Instruments) at $m/\Delta m \sim 700$. An in-house standard has been measured before measuring unknown samples to monitor the quality of the mass spectrometric measurements. International reference rock standards such as JB-2 from the Geological Survey of Japan (GSJ) were prepared with unknown samples to check for possible lithium isotope fractionation on the ion exchange columns and/or blank effects. Samples were measured with a standard-sample bracketing method using L-SVEC as a reference [40]. Lithium isotope ratios are calculated as $\delta^7Li\ (‰) = [(^7Li/^6Li)_{sample}/(^7Li/^6Li)_{standard} - 1] \times 1000$. The in-run precision of single measurements varied typically between 0.05 and 0.10‰ (2SE). Three to five individual runs were performed for each sample from which the mean and 2σ analytical uncertainty were calculated. The long-term reproducibility and precision of our in-house Li standard is $\delta^7Li = 0.94 \pm 0.14‰$ (2σ, $n=28$). Analyses of JB-2 prepared together with Mt. Shasta volcanic rocks averaged $\delta^7Li = 4.79 \pm 0.29‰$ (2σ, $n=4$) in four analytical sessions. This is in excellent agreement with published data [39,41–44].

Concentration measurements were performed on a quadrupole ICPMS VG Elemental PQ2 prior to separation and thereafter using beryllium as an internal standard for matrix element correction. The Li concentrations so determined were used to calculate yields and to reject samples with <95% recovery. We also used the PQ2 to monitor each sample for the presence of matrix elements (Na, Mg, Al, Ca, Fe) after ion-exchange chromatography. Samples with a total matrix content that exceeded 20% of the Li abundance were not used for isotope analysis. Trace element concentrations, with the exception of Li, were determined on the PQ2 using rhodium as an internal standard. The accuracy and precision of trace element analyses were checked against analysis of JB-2 (GSJ), BHVO-2 and AGV-2 (USGS). Barium contents were higher by about 10–15% relative to reference values. Accordingly, Ba abundances for tholeiites, basaltic and magnesian andesites were corrected down by 15% and for andesites and dacites down by 10%. The 2σ errors on concentration measurements were better than 5% for most elements, with some scatter for Cs (<10%).

Strontium (Sr) and neodymium (Nd) were separated following procedures of Horwitz et al. [45] and Cohen et al. [46], respectively. Strontium and Nd isotope

Table 1
Lithium concentrations and isotope compositions in Mt. Shasta and Medicine Lake lavas

Sample	Type	Li	δ^7Li	2σ	n[a]
Mt. Shasta					
85–38[b]	HAOT	6.0	3.04	0.24	1
85–51[b]	HAOT	6.3	3.02	0.62	3
82–94a[b]	BA	7.3	6.41	1.06	3
85–44[b]	BA	5.5	4.04	1.23	2
95–15[b]	BA	6.8	4.98	0.49	2
95–17[b]	BA	5.0	5.14	0.42	3
85–41b[b]	PMA	10.2	4.74	0.58	2
82–94d[b]	A	6.0	6.27	0.26	1
85–55[b]	A	11.2	2.88	0.08	1
85–3[b]	A	8.3	4.50	0.13	1
85–48b[b]	A	8.2	6.44	0.27	1
85–59[b]	A	18.4	6.35	0.15	1
82–85[b]	A	20.2	3.31	0.17	1
82–92a[b]	D	35.2	2.79	0.40	3
82–95[b]	D	28.0	5.97	0.33	2
82–91b[b]	D	9.7	5.21	0.22	1
96–1[b]	D	9.9	3.06	0.18	1
97–7[b]	D	8.3	6.38	0.33	1
83–50[b]	D	6.6	4.44	0.13	1
83–58[b]	D	10.3	2.99	0.14	1
95–13[b]	D	9.1	6.89	0.07	1
Medicine Lake					
82–72a[c]	HAOT	3.2	2.42	0.29	2
95–3[d]	HAOT	7.8	1.22	0.27	1
95–4[d]	HAOT	6.9	2.83	0.16	1
95–5[d]	HAOT	4.6	1.19	0.41	1
95–6[d]	HAOT	5.0	3.20	0.09	1
95–9[d]	HAOT	5.2	5.02	0.29	2
1665m[e]	LB	6.9	3.28	0.20	1
1672m[e]	LB	6.1	1.95	0.42	1
1399m[f]	BA	8.9	2.36	0.14	1
79–24E[f]	BA	11.4	0.93	0.30	2
Reference standards					
JB–2			4.79	0.29	4
BHVO–2			4.43	0.41	2
AGV–2			8.14	0.66	2

Li concentrations are given in ppm. Li isotope compositions expressed in per mil relative to L-SVEC standard.
HAOT — high-alumina olivine tholeiite, BA — basaltic andesite, PMA — primitive magnesian andesite, A — andesite, D — dacite, LB — Lake Basalt.
[a] number of full replicate measurements including sample dissolutions.
[b] see Grove et al. [34] for Sr, Nd and Pb isotopes and trace element geochemistry.
[c] see Baker et al. [47].
[d] see Elkins Tanton et al. [38].
[e] see Wagner et al. [37].
[f] see Kinzler et al. [36].

compositions were measured on a Nu Plasma MC-ICPMS (Nu Instruments). Masses 83 and 85 were used to correct for Kr and Rb interferences, respectively, that were <1% of the respective Sr isotope beam. The instrumental mass bias was corrected using an exponential fractionation law. The $^{87}Sr/^{86}Sr$ ratios were corrected for mass bias using $^{88}Sr/^{86}Sr=8.3752$ and $^{143}Nd/^{144}Nd$ was corrected using a $^{146}Nd/^{144}Nd$ of 0.7219. All $^{143}Nd/^{144}Nd$ ratios were normalized to the JMC-Nd standard using $^{143}Nd/^{144}Nd=0.511833$ (cross-calibrated to a ratio of 0.511858 for La Jolla standard). $^{87}Sr/^{86}Sr$ ratios were normalized to the accepted ratio of 0.710245 for the NIST SRM 987. These new Sr data are within ±0.01% (1ε unit) of previous Sr isotope data for Medicine Lake olivine tholeiite 82–72a [47] and basaltic andesite 79–24E [36].

4. Results

Lithium abundances and isotope data for Mt. Shasta and Medicine Lake lavas are presented with other radiogenic isotope data in Tables 1 and 2 (see Grove et al. [2] for Sr, Nd and Pb isotope data for the Mt. Shasta lavas). Lithium contents of olivine tholeiites and basaltic andesites are within the range reported for arc volcanics from southern Washington Cascades [21] and Central America [11] but are about half of those of subduction-related calc-alkaline lavas of the Panama arc [23]. The Li abundances range from 3.2 to 7.8 ppm in HAOTs, are between 5.0 and 11.4 ppm in BA and Lake Basalt lavas, and yield a value of 10.2 ppm for PMA sample 85–41b. Most andesites and dacites have Li concentrations ranging from 6 to 11 ppm. The δ^7Li values of HAOTs, BA lavas and PMA vary between +0.9‰ and +6.4‰ relative to L-SVEC with only slight overlap between Mt. Shasta and Medicine Lake volcanics (Fig. 1). A subset of two andesites and two dacites exhibits high Li abundances (up to 35 ppm) compared to other evolved lavas; this is paralleled by high Rb, Cs, Ba, Pb, Th and U concentrations and slightly elevated $^{87}Sr/^{86}Sr$. All andesites and dacites from Mt. Shasta have δ^7Li values between +2.8‰ and +6.9‰ which is within the range of BA lavas and HAOTs.

Table 2
Sr and Nd isotope compositions of Medicine Lake lavas

Sample	Type	$^{87}Sr/^{86}Sr$	$^{143}Nd/^{144}Nd$
82–72a	HAOT	0.703402 (11)	0.513010 (8)
95–3	HAOT	0.703457 (14)	0.512952 (8)
95–4	HAOT	0.703554 (11)	0.512917 (6)
95–5	HAOT	0.703556 (16)	0.512930 (7)
95–6	HAOT	0.703579 (13)	0.512933 (6)
95–9	HAOT	0.703480 (10)	0.512986 (9)
1665m	LB	0.703762 (13)	0.512860 (6)
1672m	LB	0.703626 (13)	0.512921 (5)
1399m	BA	0.703646 (12)	0.512891 (6)
79–24E	BA	0.703780 (11)	0.512845 (7)

Numbers in parentheses are 2σ errors and refer to the last two digits for Sr and the last digit for Nd.
HAOT — high-alumina olivine tholeiite, BA — basaltic andesite, PMA — primitive magnesian andesite, A — andesite, D — dacite, LB — Lake Basalt.

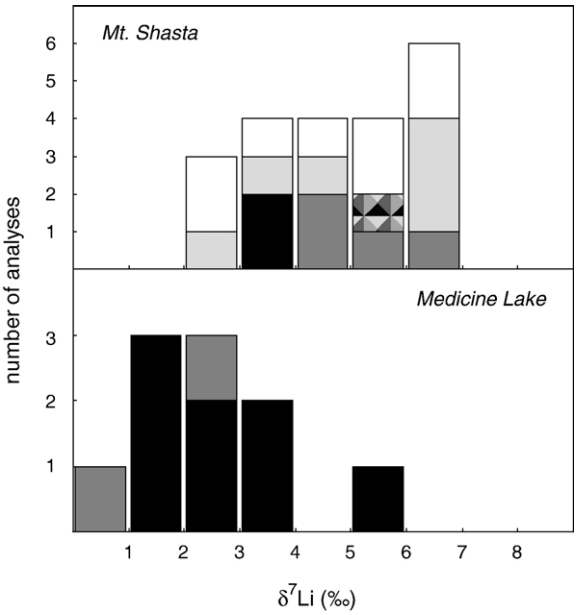

Fig. 1. Histogram of δ^7Li values in tholeiites, andesites and dacites from Mt Shasta and Medicine Lake. High-alumina olivine tholeiites are in black, basaltic andesites in dark grey, primitive magnesian andesite with pattern, andesites are in light grey and dacites are in white. Progressive enrichment in ^{7}Li is found in Mt. Shasta BA lavas, whereas BA lavas from Medicine Lake have light δ^7Li values, probably as a result of Li isotope fractionation during subduction.

Selected trace element concentrations are presented in Tables 3 and 4, respectively, and are within 5% of the abundances previously reported for these elements [2,35–37,47]. MORB-normalized patterns are remarkably similar with only subtle differences in Nb (Ta) depletion and REE pattern (Fig. 2). HAOT and BA lavas from Mt. Shasta and Medicine Lake cannot be resolved from each other in their normalized patterns.

5. Discussion

5.1. High-alumina olivine tholeiites

High pressure experiments [48] show that HAOTs from the Medicine Lake area originate from near-anhydrous melting of spinel peridotite consistent with

Table 3
Trace element concentrations in Mt. Shasta and Medicine Lake lavas

Sample	Type	Rb	Cs	Sr	Ba	Sc	Y	Zr	Hf	Nb	Ni	Co	Pb	Th	U
Mt. Shasta															
85–38	HAOT	4.9	0.10	169	117[a]	26	20.3	62	2.0	2.8	42	57	1.3	0.77	0.23
85–51	HAOT	3.5	0.10	228	123[a]	31	23.7	73	2.2	2.8	52	60	1.4	0.63	0.17
82–94a	BA	4.9	0.27	734	258[a]	30	13.8	83	1.9	4.5	138	37	5.0	2.0	0.50
85–44	BA	3.1	0.07	253	108[a]	21	12.2	47	1.5	2.1	247	56	1.2	0.46	0.17
95–15	BA	5.6	0.14	611	325[a]	22	13.1	82	1.9	3.8	245	42	3.9	1.9	0.49
95–17	BA	1.2	0.03	364	53[a]	25	18.4	70	1.6	0.9	118	40	0.79	0.33	0.10
85–41b	PMA	12.3	0.59	741	167[a]	19	10.1	83	2.7	3.5	128	64	3.5	1.9	0.61
82–94d	A	17.6	0.58	1254	338[b]	11	11.1	125	2.9	3.0	176	15	6.2	3.1	0.97
85–55	A	21.0	1.18	1023	561[b]	20	13.8	137	3.7	4.4	242	40	7.3	3.8	1.20
85–3	A	16.0	0.52	1170	291[b]	13	11.6	110	2.8	4.3	236	32	4.2	2.1	0.63
85–48b	A	13.4	0.27	1509	202[b]	12	9.7	94	2.8	3.6	187	30	3.7	2.1	0.56
85–59	A	37.3	1.97	1030	653[b]	14	11.8	160	4.1	7.6	255	32	11	6.1	1.80
82–85	A	40.7	2.49	914	609[b]	12	11.2	146	3.2	6.8	223	17	8.3	5.9	1.80
82–92a	D	57.3	4.72	498	537[b]	8	10.0	101	2.6	5.4	123	8	10	6.5	2.50
82–95	D	69.0	2.71	492	488[b]	13	14.5	131	3.2	7.3	182	15	9.5	8.7	3.00
82–91b	D	18.5	0.42	1022	275[b]	11	9.1	99	2.3	3.6	195	15	3.8	2.5	0.78
96–1	D	18.7	0.86	1098	264[b]	11	9.4	107	2.5	3.2	182	15	5.2	2.1	0.64
97–7	D	18.0	0.80	1051	286[b]	11	10.9	115	2.5	3.9	199	16	5.0	2.3	0.69
83–50	D	8.2	0.45	440	191[b]	22	14.3	73	1.6	3.9	341	31	2.7	1.0	0.34
83–58	D	17.4	0.84	1174	260[b]	11	9.2	106	3.0	3.6	186	39	5.9	2.1	0.63
95–13	D	12.8	0.62	1176	194[b]	10	7.3	84	2.0	1.8	174	14	3.8	1.7	0.51
Medicine Lake															
82–72a	HAOT	1.0	0.017	164	24[a]	26	17.1	41	1.5	1.4	494	75	0.36	0.21	0.08
95–3	HAOT	11.1	0.450	473	389[a]	31	28.1	137	2.9	6.3	456	43	3.7	1.6	0.50
95–4	HAOT	4.4	0.190	358	240[a]	27	20.3	95	2.1	6.9	98	39	2.9	1.3	0.42
95–5	HAOT	2.2	0.065	390	94[a]	32	21.9	82	1.6	6.7	123	47	6.0	0.37	0.08
95–6	HAOT	3.1	0.043	370	127[a]	25	22.6	110	2.2	10.7	133	45	0.97	0.53	0.17
95–9	HAOT	1.3	0.034	287	98[a]	25	21.1	61	1.4	2.3	187	52	0.85	0.32	0.09
1665m	LB	5.5	0.297	538	242[a]	20	14.3	69	1.6	2.8	60	28	3.0	1.3	0.35
1672m	LB	6.0	0.350	585	241[a]	23	17.2	77	1.7	3.0	41	30	2.2	0.79	0.25
1399m	BA	9.0	0.395	357	194[a]	26	21.7	97	2.1	4.3	77	37	2.7	1.1	0.37
79–24E	BA	16.3	0.810	445	241[a]	23	16.8	88	1.9	4.4	108	35	5.0	1.6	0.51
Reference standards															
JB–2		6.1	0.67	199	235[a]	49	23.0	47	1.3	0.67	19.7	38	5.3	0.31	0.17
BHVO–2		7.7	0.09	407	138[a]	30	24.8	165	4.1	19.7	126	46	1.5	1.34	0.44
AGV–2		71	1.31	712	1142[b]	14	19.0	225	4.5	15.5	20	16	13	6.7	1.76

All trace element concentrations are given in ppm.
HAOT — high-alumina olivine tholeiite, BA — basaltic andesite, PMA — primitive magnesian andesite, A — andesite, D — dacite, LB — Lake Basalt.
[a] corrected down for 15%.
[b] corrected down for 10%.

low water contents of melt inclusions in olivine [49]. Anhydrous melting has also been assumed for HAOTs from Mt. Shasta on the basis of very similar major element chemistry [2] and low pre-eruptive water contents in HAOTs from northern California Cascades [49]. Analysis of primitive HAOTs from the Cascades region has shown that the magmas underwent fractional crystallization of olivine+plagioclase and the depth of their generation increases eastwards parallel to modeled corner flow lines rather than dip of subduction [38]. The Li isotope compositions of HAOTs from Mt. Shasta give an identical δ^7Li=+3.0‰ whereas HAOTs from the Medicine Lake region range from +1.2 to +5.0‰. There is no indication from existing data that Li isotopes fractionate during partial melting or magmatic differentiation on Earth [50]. An exception might be the extensive magmatic differentiation during crystallisation of the lunar magma ocean which produced a range of cumulate sources with distinct Li isotope signatures [51]. Nevertheless, Li isotope variations observed in HAOTs in this study most likely reflect heterogeneity of the mantle below the Mt. Shasta and Medicine Lake regions. Such chemical variability of

Table 4
Rare earth element concentrations in Mt. Shasta and Medicine Lake lavas

Sample	Type	La	Ce	Pr	Nd	Sm	Eu	Gd	Tb	Dy	Ho	Er	Tm	Yb	Lu
Mt. Shasta															
85–38	HAOT	4.60	11.2	1.68	8.20	2.67	1.01	2.90	0.57	3.80	0.82	2.53	0.36	2.37	0.37
85–51	HAOT	4.74	11.9	1.90	9.30	3.22	1.26	3.40	0.62	4.24	0.90	2.81	0.41	2.66	0.38
82–94a	BA	12.0	26.0	3.53	14.3	3.55	1.14	3.03	0.46	2.60	0.52	1.47	0.23	1.47	0.21
85–44	BA	3.78	9.00	1.34	5.90	1.98	0.69	2.00	0.36	2.20	0.47	1.50	0.22	1.36	0.20
95–15	BA	16.0	35.7	4.67	18.9	4.11	1.25	3.29	0.45	2.60	0.50	1.53	0.22	1.44	0.22
95–17	BA	3.50	9.40	1.56	8.10	2.62	1.05	2.90	0.54	3.50	0.73	2.18	0.33	2.21	0.30
85–41b	PMA	10.3	23.1	3.06	12.3	2.70	0.92	2.30	0.34	1.88	0.39	1.14	0.16	1.05	0.16
82–94d	A	18.1	39.7	5.40	20.8	4.34	1.46	3.40	0.41	2.30	0.40	1.22	0.16	1.06	0.16
85–55	A	22.8	51.1	6.81	26.7	5.73	1.75	4.30	0.53	2.76	0.52	1.58	0.21	1.38	0.20
85–3	A	15.2	33.1	4.30	17.1	3.89	1.29	3.10	0.41	2.29	0.43	1.34	0.18	1.22	0.17
85–48b	A	15.6	36.1	4.77	17.9	3.47	1.20	2.95	0.37	1.93	0.37	1.11	0.14	0.97	0.14
85–59	A	28.6	57.7	7.21	27.5	5.94	1.71	4.05	0.49	2.50	0.44	1.30	0.18	1.18	0.17
82–85	A	25.1	50.9	6.30	23.8	5.08	1.52	3.79	0.47	2.34	0.45	1.26	0.17	1.14	0.16
82–92a	D	15.1	29.2	3.52	13.1	3.38	1.06	2.51	0.37	1.98	0.38	1.13	0.16	1.06	0.17
82–95	D	19.1	38.6	4.79	18.1	4.41	1.18	3.60	0.49	2.81	0.55	1.60	0.23	1.53	0.23
82–91b	D	12.8	27.2	3.50	13.9	3.21	1.05	2.56	0.35	1.92	0.37	1.06	0.15	0.94	0.14
96–1	D	12.9	27.6	3.62	14.3	3.42	1.11	2.80	0.35	1.85	0.37	1.07	0.16	0.96	0.15
97–7	D	14.3	30.9	3.98	16.0	3.63	1.18	2.90	0.40	2.12	0.42	1.20	0.17	1.10	0.16
83–50	D	7.00	15.9	2.25	10.1	2.88	1.09	2.70	0.46	2.70	0.56	1.70	0.23	1.55	0.23
83–58	D	13.3	29.0	3.75	15.0	3.40	1.11	2.70	0.35	1.90	0.36	0.99	0.14	0.93	0.15
95–13	D	9.74	21.3	2.87	11.7	2.66	0.95	2.20	0.27	1.57	0.29	0.86	0.11	0.71	0.12
Medicine Lake															
82–72a	HAOT	1.58	4.60	0.82	4.39	1.80	0.76	2.13	0.45	3.11	0.68	2.10	0.30	2.10	0.30
95–3	HAOT	11.1	25.9	3.74	16.4	4.94	1.90	4.90	0.80	5.10	1.04	3.10	0.46	3.00	0.46
95–4	HAOT	8.80	20.0	2.77	12.2	3.49	1.29	3.30	0.60	3.84	0.78	2.39	0.35	2.39	0.35
95–5	HAOT	5.95	15.1	2.23	10.7	3.21	1.25	3.60	0.61	4.10	0.86	2.60	0.37	2.51	0.38
95–6	HAOT	8.60	21.2	3.03	13.7	3.93	1.49	4.00	0.68	4.40	0.91	2.70	0.37	2.59	0.38
95–9	HAOT	3.58	9.39	1.48	7.60	2.51	1.08	3.60	0.53	3.77	0.84	2.47	0.37	2.40	0.36
1665m	LB	7.10	15.8	2.14	9.50	2.75	1.10	2.70	0.44	2.70	0.56	1.67	0.23	1.61	0.27
1672m	LB	6.85	15.8	2.30	10.5	3.18	1.40	3.20	0.52	3.20	0.64	2.02	0.27	1.90	0.27
1399m	BA	7.90	18.7	2.72	12.2	3.65	1.32	3.70	0.64	4.10	0.85	2.55	0.37	2.48	0.36
79–24E	BA	9.30	20.4	2.80	11.8	3.37	1.20	3.20	0.51	3.16	0.67	1.90	0.28	1.86	0.27
Reference standards															
JB–2		2.35	6.88	1.24	6.4	2.40	0.97	3.12	0.61	3.95	0.88	2.60	0.41	2.55	0.39
BHVO–2		15.5	38.6	5.56	24.9	6.23	2.29	6.4	1.08	5.54	1.06	2.64	0.42	2.12	0.38
AGV–2		39.4	71.7	8.6	31.3	5.8	2.04	5.6	0.69	3.6	0.71	1.95	0.26	1.69	0.27

All rare earth element concentrations are given in ppm.
HAOT — high-alumina olivine tholeiite, BA — basaltic andesite, PMA — primitive magnesian andesite, A — andesite, D — dacite, LB — Lake Basalt.

the mantle sources has been drawn from trace element models in primitive HAOTs and BAs from adjacent Lassen region [52]. There is no evidence for assimilation of granitic crust and/or contamination of HAOTs by Trinity harzburgites, inferred beneath Mt. Shasta [35]. Therefore, relative fertility of mantle wedge segments beneath Mt. Shasta and Medicine Lake [53] may account for the observed several per mil scatter in HAOTs.

HAOTs are relatively enriched in fluid mobile elements such as Pb, Sr and Li compared to MORB (Fig. 2). The enrichment of highly fluid mobile elements provides evidence for a subduction-related component in HAOTs (see also Hart [54]). This is consistent with metasomatic enrichment of this mantle segment before melt extraction. Therefore, HAOTs contain variable proportions of mantle and slab-derived Li. It has been argued that these trace element patterns provide evidence for a connection with the recent subduction volcanism in the Cascades [35,55,56]. In contrast, Hart [54] noted that radiogenic Sr isotope ratios continue to the east of the arc and seems not related to modern subduction zone volcanism. The latter is consistent with radiogenic strontium of $^{87}Sr/^{86}Sr=0.70434$ for Mt. Shasta HAOTs whereas Medicine Lake HAOTs range from 0.7032 to 0.70345.

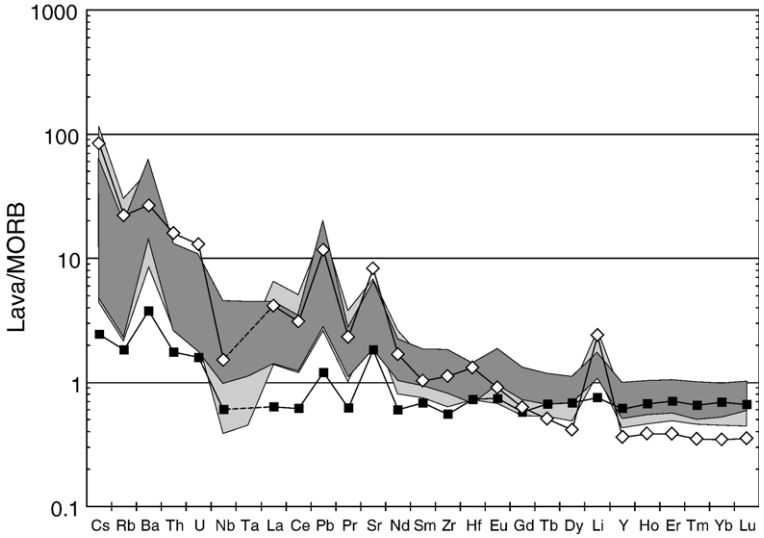

Fig. 2. Trace element patterns for HAOT and BA lavas from Mt. Shasta and Medicine Lake (not separated). The dark grey field is that of HAOTs. The most depleted HAOT lava 82–72a is plotted separately as black squares and shows a pattern that is similar to that of other samples 82–72a1 [55] and 82–72f [56] studied previously. The HAOTs from Mt. Shasta and Medicine Lake are identical in their trace element patterns. The light grey field represents BA lavas; PMA lava 85–41b is plotted separately (white diamonds). Two BA lavas and two Lake Basalt lavas from Medicine Lake cannot be resolved from Mt. Shasta BA lavas based on their trace element patterns. All lavas exhibit similar trace elements pattern with enriched Cs, Ba, Pb, Sr and Li and Nb, Ta depletion. For normalization N-MORB data from Sun and McDonough [76] are used.

At least some HAOTs seem to contain a component with high time-integrated Rb/Sr that is related to metasomatism by slab-derived fluids some time in the past. Although the timing of the enrichment in fluid mobile elements is unclear the anhydrous lavas provide evidence for an isotopically heterogeneous mantle wedge with predominant isotopically light Li beneath Medicine Lake.

5.2. Basaltic andesites and primitive magnesian andesites

The pre-eruptive H_2O contents of these lava provide constraints on the composition of the slab component and the process of melt formation. The BA lavas have high Mg #s providing evidence for equilibration with spinel peridotite [2]. Olivines with a forsterite content of ~93.6 have been reported for the primitive Mg-andesites (PMA). Experiments show that both BA lavas (85–44; [35]) and PMA (85–41b; [57]), are saturated with olivine and orthopyroxene at ~1.0 GPa and 1200 °C. The olivine crystals in the PMA are igneous and crystallized from a magma that was derived from an extremely depleted mantle source [35]. The experiments provide evidence that the major-element chemistry of BA lavas and PMA from Mt. Shasta are in equilibrium, or nearly so, with peridotites at the base of the crust [2].

Geochemical variations in primitive BA lavas from the southern Cascades have been accounted for by reactions of fluid phases with mantle wedge peridotites [53,58]. However, boron (B) abundance and isotope data place ambiguous constraints on the nature of the fluid phase in the primitive Mt. Shasta BA lavas and do not distinguish a B-depleted hydrous fluid from a H_2O-rich slab melt [59]. The major element chemistry of BA lavas and PMA is in equilibrium, or nearly so, with peridotite. However, up to 99% of the fluid-mobile trace elements such as Rb, Sr or Ba may come from the subducted oceanic lithosphere [2]. Lithium is easily mobilized from altered basalts or sediments during shallow-depth reaction with hydrothermal fluids [17] or in accretionary prisms [60]. However, during continuing subduction and change in P–T conditions, the remaining Li is more strongly bound in the slab, presumably in mineral phases such as omphacite, Ti-clinohumite and olivine [9,61], with relatively high Li abundances, generally exceeding 10 ppm. Recently, variable δ^7Li values have been reported for a suite of Mariana forearc serpentinites, the data scattering between −6.1‰ and +10.3‰ [13]. This complicates estimates of the exact Li isotope composition of slab-derived fluids.

Strontium, Nd and Pb isotope compositions provide evidence that at least two fluid-rich geochemical reservoirs were involved in the generation of Mt. Shasta lavas, one with MORB-like $^{87}Sr/^{86}Sr$ (~0.7028) and ε_{Nd} and a second with high $^{87}Sr/^{86}Sr$ (~0.7037) and low ε_{Nd} [2]. The δ^7Li of basaltic andesites from Mt. Shasta

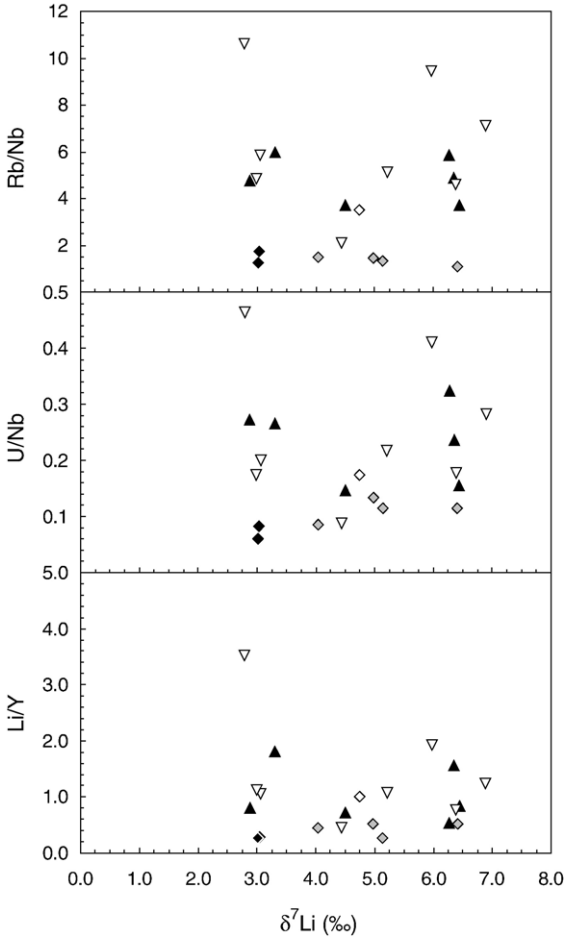

Fig. 3. Trace element ratios vs. δ^7Li values in Mt. Shasta lavas. An apparent scatter of data with no systematic behavior among diverse lava types reflects Li isotope fractionation decoupled from release of a fluid phase during dehydration. Closed diamonds — high-alumina olivine tholeiites; grey diamonds — basaltic andesites; open diamond — primitive magnesian andesite; closed triangles — andesites; reversed open triangles — dacites.

varies between +4.0‰ and +6.4‰. Both fluid-rich reservoirs exhibit high δ^7Li. This is consistent with an origin from variably altered mid-ocean ridge basalts [62] which are ^{7}Li-enriched and may show Sr isotope variation. The high-^{87}Sr/^{86}Sr fluid reservoir is unlikely to reflect detrital sediments while the upper continental crustal materials seem to be isotopically lighter, averaging δ^7Li of ~0‰ [63]. A different fluid source with δ^7Li <0.9‰ is indicated by BA lavas and Lake Basalt lavas from the Medicine Lake region. However, all BA lavas and PMA have low Rb/Nb (<3.7) and intermediate Sr/Y (16–73) and are enriched in Li over similarly compatible elements like Y or Ho (Fig. 2).

Lithium isotopes provide a tracer of near surface fractionated materials. Therefore, the most obvious explanation of the difference between Mt. Shasta and Medicine Lake lavas is distinct mantle components above the Cascadia subduction zone. However, there are several lines of evidence that this model is incorrect or at least greatly simplified.

First, the BA lava and Lake Basalt lava from the Medicine Lake region have ^{87}Sr/^{86}Sr=0.7036 and 0.7038 respectively, and cannot be distinguished from Mt. Shasta BA lava with the "sediment signature" (^{87}Sr/^{86}Sr=0.7037 to 0.7039; Table 2 and Grove et al. [2]). The latter indicates that the hydrous Mt. Shasta and Medicine Lake lava were derived from similar sources despite distinct Li isotope compositions. Second, if δ^7Li is behaving like a radiogenic tracer for crustal material in the Cascadia subduction zone, then correlations with other fluid mobile elements or element ratios, e.g. Rb, Ba or Sr isotopes, would be expected. However, Li isotopes do not correlate with any of these (Fig. 3).

A likely explanation for the difference between Mt. Shasta and Medicine Lake lavas is that Li isotopic effects are dominated by fractionation during subduction of the oceanic lithosphere. Dehydration of a subducting plate extracts heavy Li into the fluid and leaves residues that are depleted in ^{7}Li. Lithium isotope fractionation during dehydration of oceanic crust is evident from fluids of the Costa Rica decollement zone [64] and serpentine diapirs, both with δ^7Li of about +20‰. δ^7Li values of dehydration residues change during prograde metamorphism with increasing degree of dehydration. Eclogites from Trescolmen [9] and an eclogite sample from Oberkotzau, Germany [39] have negative δ^7Li values. Both provide evidence for a ^{7}Li-depleted eclogitic residue in subduction zones. The pathways of Li depletion and isotope fractionation are not expected to be constant at all pressure and temperature conditions in subduction zones. However, dehydration at low temperatures will fractionate ^{7}Li into the fluids and produce a ^{6}Li-enriched residue. Therefore, fluids that derived from the slab below ~75 km are expected to be isotopically lighter than unaltered MORB as also recently experimentally verified [65].

5.3. Andesites and dacites

Andesites (A) and dacites (D) from Mt. Shasta have been modeled as products of multiple recharge of magmatic reservoirs by parental H_2O-rich PMA magmas (e.g. 85–41) accompanied by fractional crystallization of olivine+pyroxenes+amphibole+plagioclase throughout (or within) the continental crust. Possibly some BA lava were also introduced into the system [34] and served as parent magmas. Both water content in

melt inclusions and evidence from experimental work indicate high pre-eruptive H_2O contents (up to 10 wt.%) in some evolved magmas [33]. Similar water contents have been observed in northern Cascadia [66]. Although crustal rocks are present in the area [27], Sr and Nd isotope data do not indicate contamination by continental crust. This is also endorsed by U–Th–Ra disequilibria for young volcanic rocks [67]. Andesites and dacites are therefore derived from a H_2O-rich PMA-magma by fractional crystallization and mixing with related, but more evolved magmas [34]. This mode of origin differs from that proposed for the generation of andesitic, dacitic and rhyodacitic lavas in the High Cascades where melting of amphibolitic and granulitic rocks at various crustal levels without significant mafic contributions has been suggested [68]. Average continental crust and Trinity peridotite as contaminants have been excluded based on major and trace elements [34]. Continental crust has been advocated formerly [69]. The likely contaminant has been identified as highly evolved differentiated residual liquids from long-lived magmatic systems that underwent fractional crystallization, recharge of magma and mixing [34]. Andesites and dacites show a similar range of trace element characteristics with, for example, depletion in Nb and Ta, accompanied by enrichment in Ba, Pb, Sr and Li (Fig. 4). The δ^7Li range measured for andesites and dacites is identical to the Li isotope composition of tholeiites and basaltic andesites. This precludes a voluminous contamination of andesites and dacites by old or upper crustal material and restricts its volume to less than 5% (andesites: Li=10 ppm, δ^7Li=7‰, Sr=1200 ppm, $^{87}Sr/^{86}Sr$=0.7028, continental crust: δ^7Li=0‰, Li=35 ppm [63], $^{87}Sr/^{86}Sr$=0.740, Sr=276 ppm, CC2 composition in Table 5 from Hart [54]). Although the upper continental crust appears to have δ^7Li ~0‰ [63], the Sr and Nd isotope compositions will have evolved in a manner that is distinct from those of the mantle and basaltic systems. Evolved calc-alkaline lavas of Panama arc show a considerable range in δ^7Li from +3.9‰ to +11.2‰ (Old Group in Tomascak et al. [23]). This has been ascribed to release of isotopically heavy Li from previously subduction-fertilized mantle in an environment where ridge subduction was being initiated. In contrast, adakitic lavas from the Panama arc exhibit a much more limited range in δ^7Li from +1.4‰ to +4.2‰ and may represent slab melts. Such an interpretation is broadly consistent with the model presented in this study.

A subset of four Li-rich samples (85–59, 82–85, 82–92a, 82–95) shows distinct $^{87}Sr/^{86}Sr$ ratios compared to the rest of andesites–dacites group. These samples carry a Sr isotope signature of a sediment-derived fluid-rich component [34]. Lithium abundances between 18 and 35 ppm also provide evidence for varying degrees of contamination by rhyolitic rocks. However, their δ^7Li values scatter substantially and this may reflect heterogeneity in the rhyolitic contaminant. It is possible that variability in the δ^7Li is a characteristic of this rhyolitic residuum [34].

We suggest that the mineralogy of the subducted slab does not have a large effect on the Li isotope composition

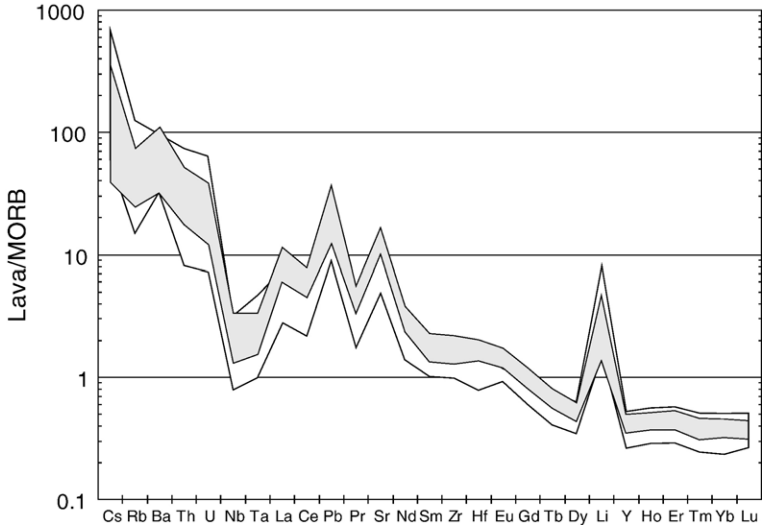

Fig. 4. Trace element patterns for andesites and dacites from Mt. Shasta. Andesites (light grey) and dacites (white) display nearly identical patterns with only subtle differences. Andesites are more homogeneous than dacites with less variable trace element ratios, e.g. $(La/Sm)_N$ or Sr/Y, however are they generally indistinguishable from dacites in N-MORB — normalized patterns.

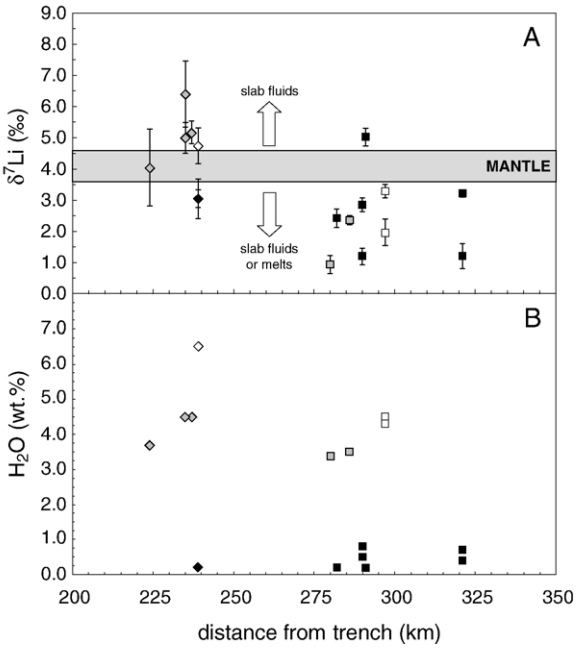

Fig. 5. Distance from the arc trench vs. δ^7Li values (panel A) and pre-eruptive water contents (panel B), respectively. Distinct Li isotope signatures are found dependent on distance from trench. A general trend of decreasing δ^7Li with increasing distance from the trench (and conversely, depth of Wadati–Benioff zone) is similar to that observed for the Izu arc [10] and has not been found in the northern Cascadia arc [21] or Kurile and Sunda arcs [19]. This has been interpreted in terms of a lack of Li isotope fractionation because Li is relatively strongly retained in subducted slab [19,21]. Similar conclusions were drawn by Moriguti et al. [20] for northeastern Japan. Diamonds — Mt. Shasta lavas (closed — HAOTs; grey — BAs; open — PMA); squares — Medicine Lake lavas (closed — HAOTs; grey — BAs; open — Lake Basalts). The mantle composition shown as a bar is defined as δ^7Li=4.1±0.5‰ as inferred from analyses of spinel lherzolites and their olivines [51]. In panel B, pre-eruptive water contents can be seen to decrease in "flux-melted" magmas as a function of distance from the trench. Significant water contents are recognized in basaltic andesites and Lake Basalt lavas from Medicine Lake.

of andesites and dacites, as these are products of multiple mixing of parental H_2O-rich magmas with fractionally crystallized lavas at crustal depths [33,34].

6. Lithium isotope fractionation in the southern Cascadia zone

The high temperatures of melting in the spinel peridotite source regions beneath Mt. Shasta and Medicine Lake (1300–1450 °C; [38]) rule out isotope fractionation of Li isotope compositions from the parental peridotite. Fluids added to the source region of HAOTs from Mt. Shasta are probably responsible for the variations in δ^7Li and represent a source material that is different from that provided by the subduction-derived fluid-rich components that were added when the hydrous basalts and basaltic andesites from Mt. Shasta and Medicine Lake formed. The BA, PMA and Lake Basalt lava displays a decrease in δ^7Li away from the arc trench (Fig. 5). This may reflect heterogeneity of the mantle wedge and continuous Li isotope fractionation as fluids are released from the slab at progressively greater depths [9].

It is a reasonable generally accepted scenario that fluids with heavy Li are injected from the subducted slab into the viscously coupled overlying mantle at shallow depth (Fig. 6). This hydrous mantle segment (probably serpentinite) is dragged down by the subducting plate [70] and metamorphosed. Just below Mt. Shasta the mantle segment begins to dehydrate as a consequence of the breakdown of serpentinite and/or chlorite at temperatures >600 °C [71]. The high temperatures of these dehydration reactions would be expected to lead to only a small fractionation of Li isotopes between the source serpentinite and the fluid. It is therefore unlikely that this mantle segment after losing its Li has very low δ^7Li. The low δ^7Li values for Mt. Shasta lavas probably were inherited during the subsequent vapor-saturated melting that occurred as the fluids ascended and encountered higher temperatures in the mantle wedge, i.e. the low-δ^7Li lava from Mt. Shasta included a mantle wedge component with relatively "normal" Li. That is, the Li is diluted with a mantle component with δ^7Li ~4‰. Therefore, δ^7Li variation observed in Mt. Shasta lava reflects both different proportions of Li derived from the slab and Li isotope heterogeneity in the mantle wedge. Further evidence of a heterogeneous mantle wedge is provided by anhydrous volcanics from the Mt. Shasta–Medicine Lake region that exhibit a large range of δ^7Li values. The complexity of this heterogeneous mixing process may explain why δ^7Li does not correlate with fluid mobile trace elements and strontium isotopes.

The H_2O-rich lava from Medicine Lake (which also has a large contribution from the slab in their incompatible element abundances) are uniformly low in δ^7Li. These lava are likely generated by vapor-saturated melting in the mantle wedge as the slab-derived fluids ascend. That the metamorphosed subducted slab contains reasonable amounts of Li has been recently shown [61]. In particular mineral phases such as staurolite [72], serpentine, phengite, chlorite and Ti-clinohumite can hold high Li abundances. Breakdown of those minerals that are H_2O-rich such as lawsonite or phengite may occur in subducted metamorphosed oceanic crust just beneath Medicine Lake. In addition, breakdown of serpentine in the subducted oceanic slab can be an effective source of Li at Medicine Lake. Such fluids will be isotopically light because heavy Li is lost

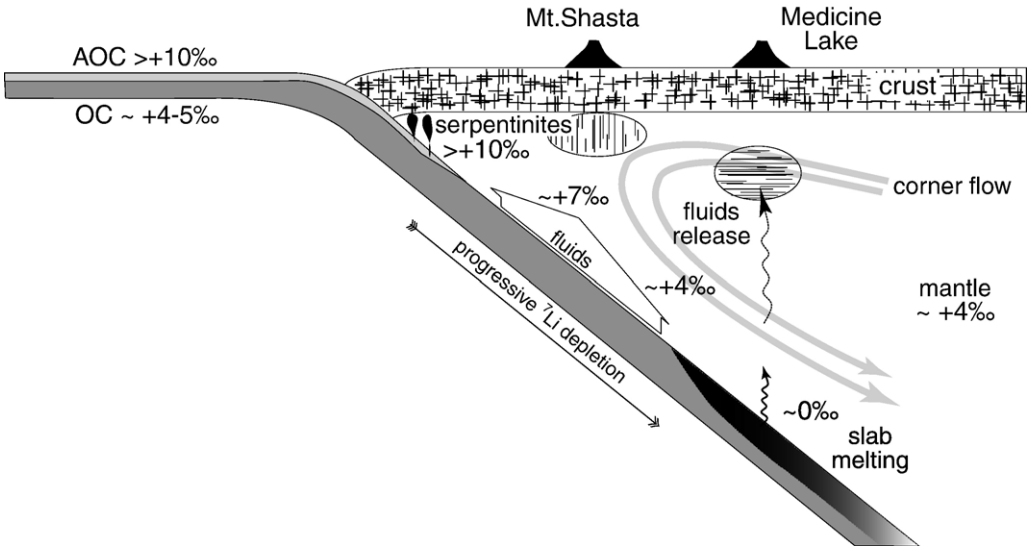

Fig. 6. Schematic figure of evolution of Li isotopes in the southern Cascadia subduction zone. Altered oceanic crust (AOC) provides source of heavy Li isotope input into the subduction zone due to ^{7}Li being preferentially adsorbed in secondary clay minerals. This Li is easily released during low-T events just after passing the arc trench. Overlying serpentinite diapirs become isotopically heavy. Progressive ^{7}Li depletion in successive steps of slab dehydration and/or slab melting is reflected in lighter Li isotope composition of BA lavas further away from the trench. HAOTs from both Mt. Shasta (with a source located just beneath the base of the continental crust, depicted as a vertically lined oval) and Medicine Lake (horizontally patterned oval indicating a deeper source of these HAOTs) represent near-anhydrous melting of spinel peridotites. Slightly different δ^{7}Li values mirror heterogeneity of the mantle segments beneath the two volcanoes.

at shallow depths causing metasomatic overprinting of the overlying mantle wedge with predominantly heavy Li. Thus, progressive dehydration reactions with the accompanying higher temperatures deeper in the downgoing slab causes the distinct δ^{7}Li observed in Mt. Shasta and Medicine Lake basaltic andesites.

Studies of eclogites from Trescolmen, Switzerland [9] and Oberkotzau, Germany [39] have revealed negative δ^{7}Li values. Fluids derived from such an eclogitic source are Li rich and expected to be light [9] because the fractionation between rock and fluid is small at high temperatures. Therefore, the data are consistent with the Wadati–Benioff zone being at greater depth and higher temperature below Medicine Lake than Mt. Shasta. The isotope fractionation in subduction zones would explain why Li isotopes do not correlate with fluid mobile trace elements and strontium isotopes. Such a decoupling has also been described for oceanic arcs [11,19] and seems to be a characteristic of most arc magmas.

7. Comparison with other arcs

Lithium isotopes have been studied in several arcs. However, only the Izu arc [10] and the southern Cascades (this study) show a decrease in δ^{7}Li values with increasing distances from the trench (or depth of the slab). These two arcs deviate from the other localities by abundant proportions of basalts (Fig. 7). For the Izu arc a mixing model has been proposed in which mantle wedge Li mixes with slab-derived Li [10]. The fluids have a signature mainly of altered oceanic crust. Such a mixing model is consistent with a study on trace elements and radiogenic isotopes by Hochstaedter et al. [73]. However, the model [10] relies on a mantle end member that has $\delta^{7}\mathrm{Li} \approx 0$ to +2‰ which is inconsistent with the vast majority of oceanic basalts and unmetasomatised peridotite xenoliths. Therefore, continuous Li isotope fractionation in the slab during subduction and an interpretation of the light end member being a slab signature seems to provide a more satisfactory explanation of the data for the Izu arc and the southern Cascades.

For andesitic lavas from northeastern Japan a slightly smaller range of δ^{7}Li values from +2.0 to +4.4‰ is reported but no systematic variation across the arc has been detected [20]. The subducted slab in northeastern Japan sinks with a dip angle of ~30° into the mantle whereas the dip angle for the Izu arc is ~50°. The different geometry and a higher temperature at the top of subducting slab in the northeastern Japan [20] may result in a dehydration of the slab at very shallow, crustal levels which are not sampled by the volcanism. It may be that in northern Japan only Li from a ^{7}Li-depleted slab is incorporated in subduction zone lavas. Therefore,

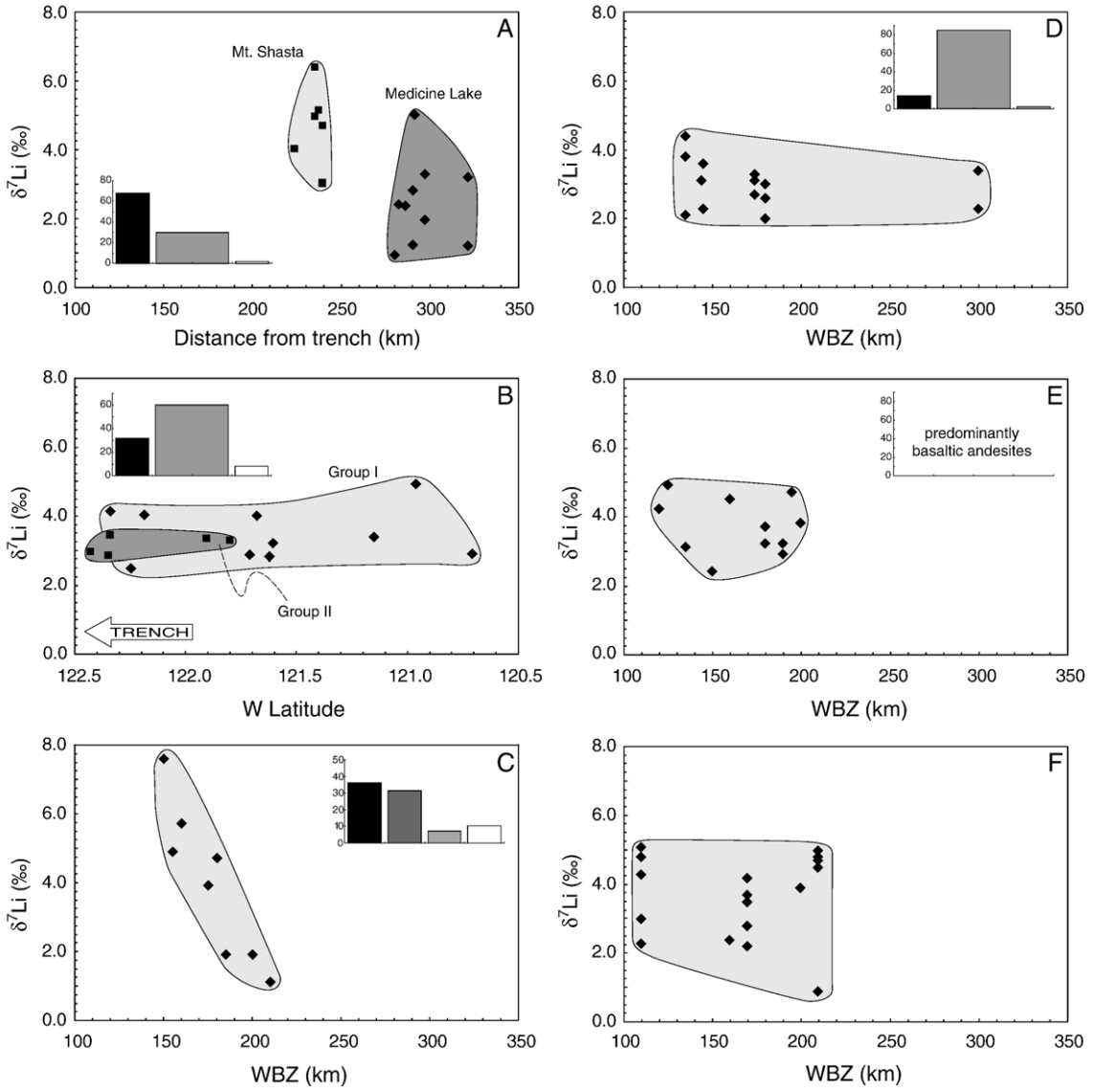

Fig. 7. Comparison of Li isotope profiles of various arcs. Lithium isotopes fractionate strongly with increasing distances (or increasing depth of Wadati–Benioff zone) from the arc trench in northern California Cascades (A) and in Izu arc (C) with predominantly basaltic volcanism [7]. On the other hand, arcs with prevalent basalt andesitic and andesitic lavas show across-arc patterns of δ^7Li values that are similar among these latter settings, i.e. restricted invariant range of δ^7Li values. A — Li isotope data from Mt. Shasta and Medicine Lake (this study), B — southern Washington Cascades (see [21] for distinctions between Group I and II), C — Izu arc [10], D — northeastern Japan arc [20], E — Kurile arc [19], F — Sunda arc [19]. Symbols are plotted irrespective of the petrologic evaluation and major element chemistry of corresponding samples. Insets: basalts are in black, basaltic and acid andesites are in dark grey and dacites are in white. Inset 7C: basaltic andesites are in dark grey and acid andesites are in light grey. Note the variations of relative proportions of major magma types in the insets [7]. WBZ — depth of Wadati–Benioff zone.

very heavy Li isotope ratios of up to 7‰ are missing. Indeed, Li–Pb isotope modeling shows that δ^7Li of slab-derived fluid and mantle wedge end members are potentially very similar resulting in lack of Li isotope fractionation during continuous subduction. A convex-upward trend of Li/Y was observed across the northeastern Japan arc and was explained by the possible influence of lawsonite breakdown [20]. This could be a consequence of shallower subduction and thus, different P–T conditions for northeastern Japan compared to Izu arc. Whether this could influence the δ^7Li path across the arc is presently unclear. A concave-upward profile of δ^{11}B across the northeastern Japan arc has been explained by involving tourmaline as a minor mineral phase that carries a substantial portion of the boron in the subducted slab [20].

Across the southern Washington Cascadia δ^7Li values of tholeiites to basaltic andesites range from +2.5 to +4.2‰ and are randomly distributed across the arc [21] which is distinct from the Li isotope patterns observed in lavas from this study. The fluid-mobile element abundances decrease from the forearc lavas towards the backarc. A corresponding effect on Li isotopes is not observed but B isotopes change systematically across the arc. It has been suggested that this is because Li is retained in the subducted slab more efficiently than B. Such an inference is in good agreement with previous observations made for other arc settings [19,20]. Hence, the Li isotope signatures in these lavas may represent the composition of the mantle wedge because there has been only a small input of isotopically distinct fluids from the slab [21].

Lithium isotope compositions of basaltic andesites and andesites in the Kurile arc range from +2.4 to +4.9‰ and are randomly distributed across the arc [19]. In contrast, B isotope ratios vary systematically with the distance to the trench [74]. It has been suggested that this is either due to very low Li contents in fluids or Li has been removed from fluids by interaction with minerals in the mantle wedge [19]. Apart from one sample, tholeiites and high-K alkali lavas of the Sunda arc display a narrow range of δ^7Li values from +2.1 to +5.1‰ [19]. This range is observed in lavas from southern Washington Cascades, Kurile and northeastern Japan arc. Mixing of isotopically heterogeneous mantle Li and a homogeneous slab-derived Li in fluids or melts is proposed for the observed B/Be and Sr–Nd–Pb isotope systematics in Sunda arc [75]. Possible explanations for the distinct Li isotope patterns in arcs involve either Li-poor slab fluids or removal of Li from the fluids by interaction in the mantle wedge [19]. In the first case, Li would be retained in the slab. Indeed, some evidence is found for such behaviour of Li during subduction (see Sections 5.2 and 6, respectively). This Li would not contribute significantly to the Li isotope budget of arc volcanics [19]. In the latter case, Li is sequestered in rims of minerals in the mantle wedge. Decoupling of Li and B isotope patterns indicates a chromatographic separation of Li isotopes as fluids percolate through the mantle wedge. This may erase the slab signature of a moderately incompatible element like Li [19] but not that of highly incompatible element like B.

In conclusion, the dip angle and the temperatures in subduction zones will affect the extent of dehydration in the subducting slab. Most ^{7}Li may be lost into the crust where subduction is shallow. In only two locations do Li isotopes show an inverse correlation with depth of Wadati–Benioff zone (or distance from trench). In these arcs, basalts are the dominant lava type. As discussed above, arcs dominated by basalts provide evidence that Li isotopes continuously fractionate in the slab during subduction. In contrast, Pb isotopes and other radiogenic tracers provide evidence that ascending fluids or melts interact and mix with distinct components in the mantle wedge.

8. Conclusions

1) High-alumina olivine tholeiites are near-anhydrous melts of spinel peridotites. Lithium isotopes are not fractionated during melting and most likely reflect Li isotope composition of the uppermost mantle beneath Mt. Shasta.
2) Lithium in the hydrous BA lavas in the Mt. Shasta region is heavy whereas BA lavas and basalts from Medicine Lake have isotopically light Li providing evidence for isotope fractionation during subduction of the lithospheric slab.
3) Basaltic andesites exhibit the same δ^7Li range as andesites and dacites from Mt. Shasta reflecting the composition of the mantle source. Thus, our data provide further evidence that solely magmatic differentiation processes are not fractionating Li isotopes.

Acknowledgement

We are indebted to Irene Ivanov-Bucher for her help with the sample preparation, Darrell Harrison for his careful reading of early versions of the manuscript, Felix Oberli for technical assistance on Nu1700 and Marcus Gutjahr for his help with Sr and Nd isotope analysis. Lui-Heung Chan, James Gill, Bill Leeman and Paul Tomascak are acknowledged for their valuable information. We are grateful to Paul Tomascak for detailed and insightful review, Tim Elliott for offline comments to the manuscript and David Price for editorial handling. ETH and Swiss Nationalfonds (SNF) supported this study.

Appendix A. Supplementary data

Supplementary data associated with this article can be found, in the online version, at doi:10.1016/j.epsl.2006.08.019.

References

[1] Y. Tatsumi, S. Maruyama, Boninites and high-Mg andesites: tectonics and petrogenesis, in: A.J. Crawford (Ed.), Boninites, Chapman and Hall, New York, 1989, pp. 50–71.

[2] T.L. Grove, S.W. Parman, S.A. Bowring, R.C. Price, M.B. Baker, The role of an H_2O-rich fluid component in the generation of primitive basaltic andesites and andesites from the Mt. Shasta region, N California, Contrib. Mineral. Petrol. 142 (2002) 375–396.
[3] P.B. Kelemen, Genesis of high Mg andesites and the continental crust, Contrib. Mineral. Petrol. 120 (1995) 1–19.
[4] R.W. Kay, Aleutian magnesian andesites: melts from subducted Pacific Ocean crust, J. Volcanol. Geotherm. Res. 4 (1978) 117–132.
[5] G.M. Yogodzinski, R.W. Kay, O.N. Volynets, A.V. Koloskov, S.M. Kay, Magnesian andesite in the western Aleutian Komandorsky region: implications for slab melting and processes in the mantle wedge, Geol. Soc. Amer. Bull. 107 (1995) 505–519.
[6] F. Dorendorf, U. Wiechert, G. Wörner, Hydrated sub-arc mantle: a source for the Klyuchevskoy volcano, Kamchatka/Russia, Earth Planet. Sci. Lett. 175 (2000) 69–86.
[7] J.B. Gill, Orogenic Andesites and Plate Tectonics, Springer–Verlag, Berlin, 1981. 391 pp.
[8] T.L. Grove, R.J. Kinzler, Petrogenesis of andesites, Annu. Rev. Earth Planet. Sci. 14 (1986) 417–454.
[9] T. Zack, P.B. Tomascak, R.L. Rudnick, C. Dalpé, W.F. McDonough, Extremely light Li in orogenic eclogites: the role of isotope fractionation during dehydration in subducted oceanic crust, Earth Planet. Sci. Lett. 208 (2003) 279–290.
[10] T. Moriguti, E. Nakamura, Across-arc variation of Li isotopes in lavas and implication for crust/mantle recycling at subduction zones, Earth Planet. Sci. Lett. 163 (1998) 167–174.
[11] L.H. Chan, W.P. Leeman, C.-F. You, Lithium isotopic composition of Central American Volcanic Arc lavas: implications for modification of subarc mantle by slab-derived fluids: correction, Chem. Geol. 182 (2002) 293–300.
[12] S. Decitre, E. Deloule, L. Reisberg, R.H. James, P. Agrinier, C. Mével, Behavior of Li and its isotopes during serpentinization of oceanic peridotites, G-cubed 3 (2002), doi:10.1029/2001GC000178.
[13] L.D. Benton, J.G. Ryan, I.P. Savov, Lithium abundance and isotope systematics of forearc serpentinites, Conical Seamount, Mariana forearc: insights into the mechanics of slab-mantle exchange during subduction, G-cubed 5 (2004), doi:10.1029/2004GC000708 (paper number Q08J12).
[14] L.H. Chan, J.C. Alt, D.A.H. Teagle, Lithium and lithium isotope profiles through the upper oceanic crust: a study of seawater–basalt exchange at ODP sites 504B and 896A, Earth Planet. Sci. Lett. 201 (2002) 187–201.
[15] L.H. Chan, J.M. Edmond, G. Thompson, K. Gillis, Lithium isotopic composition of submarine basalts: implication for the lithium cycle in the oceans, Earth Planet. Sci. Lett. 108 (1992) 151–160.
[16] R.H. James, D.E. Allen, W.E. Seyfried Jr., An experimental study of alteration of oceanic crust and terrigenous sediments at moderate temperatures (51 to 350°C): insights as to chemical processes in near-shore ridge-flank hydrothermal systems, Geochim. Cosmochim. Acta 67 (2003) 681–691.
[17] W.E.J. Seyfried, X. Chen, L.H. Chan, Trace element mobility and lithium isotope exchange during hydrothermal alteration of seafloor weathered basalt: an experimental study at 350°C, 500 bars, Geochim. Cosmochim. Acta 62 (1998) 949–960.
[18] C. Bouman, T. Elliott, P.Z. Vroon, Lithium inputs to subduction zones, Chem. Geol. 212 (2004) 59–79.
[19] P.B. Tomascak, E. Widom, L.D. Benton, S.L. Goldstein, J.G. Ryan, The control of lithium budgets in island arcs, Earth Planet. Sci. Lett. 196 (2002) 227–238.
[20] T. Moriguti, T. Shibata, E. Nakamura, Lithium, boron and lead isotope and trace element systematics of Quaternary basaltic volcanic rocks in northeastern Japan: mineralogical controls on slab-derived fluid composition, Chem. Geol. 212 (2004) 81–100.
[21] W.P. Leeman, S. Tonarini, L.H. Chan, L.E. Borg, Boron and lithium isotopic variations in a hot subduction zone — the southern Washington Cascades, Chem. Geol. 212 (2004) 101–124.
[22] L.H. Chan, W.P. Leeman, C.-F. You, Lithium isotopic composition of Central American Volcanic Arc lavas: implications for modification of subarc mantle by slab-derived fluids, Chem. Geol. 160 (1999) 255–280.
[23] P.B. Tomascak, J.G. Ryan, M.J. Defant, Lithium isotope evidence for light element decoupling in the Panama subarc mantle, Geology 28 (2000) 507–510.
[24] Y. Nishio, S. Nakai, J. Yamamoto, H. Sumino, T. Matsumoto, V.S. Prikhod'ko, S. Arai, Lithium isotopic systematics of the mantle-derived ultramafic xenoliths: implications for EM1 origin, Earth Planet. Sci. Lett. 217 (2004) 245–261.
[25] G.S. Fuis, J.J. Zucca, W.D. Mooney, B. Milkereit, A geologic interpretation of seismic-reflection results in northern California, Geol. Soc. Amer. Bull. 98 (1987) 53–65.
[26] D. Wilson, Tectonic history of the Juan de Fuca ridge over the last 40 million years, J. Geophys. Res. 93 (1988) 11863–11876.
[27] J.J. Zucca, G.S. Fuis, B. Milkereit, W.D. Mooney, R.D. Catchings, Crustal structure of Northeastern California, J. Geophys. Res. 91 (1986) 7359–7382.
[28] R.A. Harris, H.M. Iyer, P.B. Dawson, Imaging the Juan de Fuca plate beneath southern Oregon using teleseismic P wave residuals, J. Geophys. Res. 96 (1991) 19879–19889.
[29] H.M. Benz, G. Zandt, D.H. Oppenheimer, Lithospheric structure of northern California from teleseismic images of the upper mantle, J. Geophys. Res. 97 (1992) 4791–4807.
[30] N.L. Green, D.L. Harry, On the relationship between the subducted slab age and arc basalt petrogenesis, Cascadia subduction system, North America, Earth Planet. Sci. Lett. 171 (1999) 367–381.
[31] R.L. Christiansen, F.J. Kleinhampl, R.J. Blakely, E.T. Tuchek, F.L. Johnson, M.D. Conyac, Resource appraisal of the Mt. Shasta wilderness study area, open-file report, U.S. Geol. Surv. (1977) 77–250.
[32] A.T. Anderson, Evidence for a picritic, volatile-rich magma beneath Mt. Shasta, California, J. Petrol. 15 (1974) 243–267.
[33] T.L. Grove, L.T. Elkins Tanton, S.W. Parman, N. Chatterjee, O. Müntener, G.A. Gaetani, Fractional crystallization and mantle-melting controls on calc-alkaline differentiation trends, Contrib. Mineral. Petrol. 145 (2003) 515–533.
[34] T.L. Grove, M.B. Baker, R.C. Price, S.W. Parman, L.T. Elkins Tanton, N. Chatterjee, O. Müntener, Magnesian andesite and dacite lavas from Mt. Shasta, northern California: products of fractional crystallization of H_2O-rich mantle melts, Contrib. Mineral. Petrol. 148 (2005) 542–565.
[35] M.B. Baker, T.L. Grove, R.C. Price, Primitive basalts and andesites form the Mt. Shasta region, N.California: products of varying melt fraction and water content, Contrib. Mineral. Petrol. 118 (1994) 111–129.
[36] R.J. Kinzler, J.M. Donnelly-Nolan, T.L. Grove, Late Holocene hydrous mafic magmatism at the Paint Pot Crater and Callahan flows, Medicine Lake Volcano, N. California and the influence of H_2O in the generation of silicic magma, Contrib. Mineral. Petrol. 138 (2000) 1–16.
[37] T.P. Wagner, J.M. Donnelly-Nolan, T.L. Grove, Evidence of hydrous differentiation and crystal accumulation in the low-

MgO, high-Al_2O_3 Lake Basalt from Medicine Lake volcano, California, Contrib. Mineral. Petrol. 121 (1995) 201–216.
[38] L.T. Elkins Tanton, T.L. Grove, J.M. Donnelly-Nolan, Hot, shallow mantle melting under the Cascades volcanic arc, Geology 29 (2001) 631–634.
[39] T. Magna, U.H. Wiechert, A.N. Halliday, Low-blank separation and isotope ratio measurement of small samples of lithium using multiple-collector ICPMS, Int. J. Mass Spectrom. 239 (2004) 67–76.
[40] G.D. Flesch, A.R. Anderson, H.J. Svec, A secondary isotopic standard for $^6Li/^7Li$ determinations, Int. J. Mass Spectrom. Ion Phys. 12 (1973) 265–272.
[41] T. Moriguti, E. Nakamura, High-yield lithium separation and the precise isotopic analysis for natural rock and aqueous samples, Chem. Geol. 145 (1998) 91–104.
[42] P.B. Tomascak, R.W. Carlson, S.B. Shirey, Accurate and precise determination of Li isotopic compositions by multi-collector sector ICP-MS, Chem. Geol. 158 (1999) 145–154.
[43] L.H. Chan, A.F. Frey, Lithium isotope geochemistry of the Hawaiian plume: results from the Hawaii Scientific Drilling Project and Koolau volcano, G-cubed 4 (2003), doi:10.1029/2002GC000365 (paper number 8707).
[44] A.B. Jeffcoate, T. Elliott, A. Thomas, C. Bouman, Precise, small sample size determinations of lithium isotopic compositions of geological reference materials and modern seawater by MC-ICP-MS, Geostand. Geoanal. Res. 28 (2004) 161–172.
[45] E.P. Horwitz, R. Chiarizia, M.L. Dietz, A novel strontium-selective extraction chromatographic resin, Solv. Extr. Ion Exch. 10 (1992) 313–336.
[46] A.S. Cohen, R.K. O'Nions, R. Siegenthaler, W.L. Griffin, Chronology of the pressure–temperature history recorded by a granulite terrain, Contrib. Mineral. Petrol. 98 (1988) 303–311.
[47] M.B. Baker, T.L. Grove, R.J. Kinzler, J.M. Donnelly-Nolan, G.A. Wandless, Origin of compositional zonation (high-alumina basalt to basaltic andesite) in the Giant Crater lava field, Medicine Lake Volcano, Northern California, J. Geophys. Res. 96 (1991) 21819–21842.
[48] K.S. Bartels, R.J. Kinzler, T.L. Grove, High pressure phase relations of primitive high-alumina basalts from Medicine Lake, northern California, Contrib. Mineral. Petrol. 108 (1991) 253–270.
[49] T.W. Sisson, G.D. Layne, H_2O in basalt and basaltic andesite glass inclusions from four subduction-related volcanoes, Earth Planet. Sci. Lett. 117 (1993) 619–635.
[50] P.B. Tomascak, F. Tera, R.T. Helz, R.J. Walker, The absence of lithium isotope fractionation during basalt differentiation: new measurements by multicollector sector ICP-MS, Geochim. Cosmochim. Acta 63 (1999) 907–910.
[51] T. Magna, U. Wiechert, A.N. Halliday, New constraints on the lithium isotope compositions of the Moon and terrestrial planets, Earth Planet. Sci. Lett. 243 (2006) 336–353.
[52] M.A. Clynne, L.E. Borg, Olivine and chromian spinel in primitive calc-alkaline and tholeiitic lavas from the southernmost Cascade range, California: a reflection of relative fertility of the source, Can. Mineral. 35 (1997) 453–472.
[53] L.E. Borg, M.A. Clynne, T.D. Bullen, The variable role of slab-derived fluids in the generation of a suite of primitive calc-alkaline lavas from the southernmost Cascades, California, Can. Mineral. 35 (1997) 425–452.
[54] W.K. Hart, Chemical and isotopic evidence for mixing between depleted and enriched mantle, northwestern U.S.A. Geochim. Cosmochim. Acta 49 (1985) 131–144.
[55] J.M. Donnelly-Nolan, D.E. Champion, T.L. Grove, M.B. Baker, J.E. Taggart Jr., P.E. Bruggman, The Giant Crater lava field: geology and geochemistry of a compositionally zoned, high-alumina basalt to basaltic andesite eruption at Medicine Lake Volcano, California, J. Geophys. Res. 96 (1991) 21843–21863.
[56] C.R. Bacon, P.E. Bruggman, R.L. Christiansen, M.A. Clynne, J.M. Donnelly-Nolan, W. Hildreth, Primitive magmas at five Cascade volcanic fields: melts from hot, heterogeneous sub-arc mantle, Can. Mineral. 35 (1997) 397–423.
[57] S.W. Parman, Petrology and geochemistry of high-degree mantle melts, PhD thesis, MIT Cambridge, Massachusetts, 2001.
[58] L.E. Borg, A.D. Brandon, M.A. Clynne, R.J. Walker, Re–Os isotopic systematics of primitive lavas from the Lassen region of the Cascade arc, California, Earth Planet. Sci. Lett. 177 (2000) 301–317.
[59] E.F. Rose, N. Shimizu, G.D. Layne, T.L. Grove, Melt production beneath Mt. Shasta from boron data in primitive melt inclusions, Science 293 (2001) 281–283.
[60] C.-F. You, L.H. Chan, A.J. Spivack, J.M. Gieskes, Lithium, boron and their isotopes in sediments and pore waters of Ocean Drilling Program Site 808, Nankai trough: implications for fluid expulsion in accretionary prisms, Geology 23 (1995) 37–40.
[61] M. Scambelluri, O. Müntener, L. Ottolini, T.T. Pettke, R. Vannucci, The fate of B, Cl and Li in the subducted oceanic mantle and in the antigorite breakdown fluids, Earth Planet. Sci. Lett. 222 (2004) 217–234.
[62] P.B. Tomascak, Developments in the understanding and application of lithium isotopes in the earth and planetary sciences, Rev. Mineral. Geochem. 55 (2004) 153–195.
[63] F.-Z. Teng, W.F. McDonough, R.L. Rudnick, C. Dalpé, P.B. Tomascak, B.W. Chappell, S. Gao, Lithium isotopic composition and concentration of the upper continental crust, Geochim. Cosmochim. Acta 68 (2004) 4167–4178.
[64] L.H. Chan, M. Kastner, Lithium isotopic composition of pore fluids and sediments in the Costa Rica subduction zone: implications for fluid processes and sediment contribution to the arc volcanoes, Earth Planet. Sci. Lett. 183 (2000) 275–290.
[65] B. Wunder, A. Meixner, R.L. Romer, W. Heinrich, Temperature-dependent isotopic fractionation of lithium between clinopyroxene and high-pressure hydrous fluids, Contrib. Mineral. Petrol. 151 (2006) 112–120.
[66] J. Blundy, K. Cashman, Ascent-driven crystallization of dacite magmas at Mount St. Helens, 1980–1986, Contrib. Mineral. Petrol. 140 (2001) 631–650.
[67] A.M. Volpe, ^{238}U–^{230}Th–^{226}Ra disequilibrium in young Mt. Shasta andesites and dacites, J. Volcanol. Geotherm. Res. 53 (1992) 227–238.
[68] R.M. Conrey, P.R. Hooper, P.B. Larson, J. Chelsey, J. Ruiz, Trace element and isotopic evidence for two types of crustal melting beneath a High Cascade volcanic center, Mt. Jefferson, Oregon, Contrib. Mineral. Petrol. 141 (2001) 710–732.
[69] S. Newman, J.D. Macdougall, R.C. Finkel, Petrogenesis and ^{230}Th–^{238}U disequilibrium at Mt.Shasta, California, and in the Cascades, Contrib. Mineral. Petrol. 93 (1986) 195–206.
[70] T. Elliott, A. Jeffcoate, C. Bouman, The terrestrial Li isotope cycle: light-weight constraints on mantle convection, Earth Planet. Sci. Lett. 220 (2004) 231–245.
[71] P. Ulmer, V. Trommsdorff, Serpentine stability to mantle depths and subduction-related magmatism, Science 268 (1995) 858–861.

[72] B.L. Dutrow, M.J. Holdaway, R.W. Hinton, Lithium in staurolite and its petrologic significance, Contrib. Mineral. Petrol. 94 (1986) 496–506.
[73] A. Hochstaedter, J. Gill, R. Peters, P. Broughton, P. Holden, B. Taylor, Across-arc geochemical trends in the Izu–Bonin arc: contributions from the subducting slab, G-cubed 2 (2001) (paper number 2000GC000105).
[74] T. Ishikawa, F. Tera, Source, composition and distribution of the fluid in the Kurile mantle wedge: Constraints from across-arc variations of B/Nb and B isotopes, Earth Planet. Sci. Lett. 152 (1997) 123–138.
[75] C.M.H. Edwards, J.D. Morris, M.F. Thirlwall, Separating mantle from slab signatures in arc lavas using B/Be and radiogenic isotope systematics, Nature 362 (1993) 530–533.
[76] S.-S. Sun, W.F. McDonough, Chemical and isotopic systematics of oceanic basalts: implications for mantle composition and processes, in: A.D. Saunders, M.J. Norry (Eds.), Magmatism in the ocean basins, Geol. Soc. Spec. Publ. 42, Blackwell Scientific Publ., London, 1989, pp. 313–345.